10-1992

# Hydrodynamic Instability of Chemical Waves

D. A. Vasquez

J. W. Wilder

Boyd F. Edwards
*Utah State University*



Recommended Citation
"Hydrodynamic instability of chemical waves," D. A. Vasquez, J. W. Wilder, and B. F. Edwards, J. Chem. Phys. 98, 2138 (1993) [33].

# Hydrodynamic instability of chemical waves

Desiderio A. Vasquez
*Department of Physics, West Virginia University, PO Box 6315, Morgantown, West Virginia 26506-6315*

Joseph W. Wilder
*Department of Mathematics, West Virginia University, PO Box 6310, Morgantown, West Virginia 26506-6310*

Boyd F. Edwards
*Department of Physics, West Virginia University, PO Box 6315, Morgantown, West Virginia 26506-6315*

(Received 11 August 1992; accepted 21 October 1992)

We present a theory for the transition to convection for flat chemical wave fronts propagating upward. The theory is based on the hydrodynamic equations and the one-variable reaction-diffusion equation that describes the chemical front for the iodate–arsenous acid reaction. The reaction term involves the reaction rate constants and the chemical composition of the mixture. This allows the discussion of the effects of the different chemical variables on the transition to convection. We have studied perturbations of different wavelengths on an unbounded flat chemical front and found that for wavelengths larger than a critical wavelength ($\lambda > \lambda_c$) the perturbations grow in time, while for smaller wavelengths the perturbations diminish. The critical wavelength depends not only on the density difference between the unreacted and reacted fluids, but also on the speed and thickness of the chemical front.

## I. INTRODUCTION

In experiments on the iodate–arsenous acid reaction, a convectionless flat chemical front propagates upward in a cylinder of diameter less than 0.94 mm, while for diameters equal to 1.8 mm or larger, the front is curved and moves faster than the flat front.[1,2] When the front propagates downward, the front is flat for all diameters and has the same speed as the flat front moving upward. The increase in speed and change in curvature indicates the presence of convection. This is a consequence of having the reacted fluid of lower density underneath the unreacted fluid of higher density.

A previous theory of the transition to convection in autocatalytic reaction fronts[3,4] described the chemical wave propagation in terms of the eikonal relation[5,6] involving the normal speed of the front ($c$), the flat front speed ($c_0$), and the front curvature ($\mathcal{K}$): $c = c_0 + D\mathcal{K}$, where $D$ is the molecular diffusivity. In this theory, the front has zero thickness, the fluid pressure and velocities are related by jump conditions across the front, and all the chemistry is contained in the eikonal relation. The chemical composition determines $c_0$ (Ref. 7) and the density difference between the unreacted and reacted fluids. These quantities are external parameters to the theory that have to be determined from experiments or from another theoretical model. The eikonal relation provides the mechanism which stabilizes the front as it tends to speed up the valleys and slow down the hills as they deviate from the flat front. This relation was derived from a reaction–diffusion equation and has been successfully applied in other chemical wave problems, such as spiral waves in the Belousov–Zhabotinskii reaction.[8] However, it is still an approximation that requires a very thin front, and consequently it cannot be used to study the hydrodynamic stability of the front as its thickness changes. To include these effects in the theory, we need to incorporate the full reaction–diffusion equation from which the eikonal relation was derived.

Experiments on propagating fronts for the arsenous acid system performed in petri dishes established the dependence of the front speed on the chemical composition of the mixture.[9] The front velocity varies with the concentration of iodate or the acidity of the solution. These experiments were successfully described by a one variable reaction–diffusion equation whose analytical solution relates the velocity and thickness of the front to the chemical concentrations. This reaction–diffusion model is valid for mixtures with an excess of arsenous acid. For excess iodate, the reaction is more complicated. In this paper we concentrate on the simpler case of excess arsenous acid. A detailed study of the hydrodynamic instability should also incorporate the effects of the exothermicity of the reaction. Nevertheless, it was shown[10] that the thermal thickness of the front is much larger than the critical wavelength for the onset of convection. Consequently, it can be considered that the fluid above the front has the same temperature as the fluid below the front. This argument is justified by a previous calculation[11] that includes the thermal effects explicitly and shows that the results can be approximated by the limit of infinite thermal diffusivity. This limit amounts to fixing the temperature of the unreacted fluid at the higher temperature of the reacted fluid. Thus the difference in density between the unreacted and reacted fluids is due only to the differences in their compositions. In the present work, we couple the corresponding reaction–diffusion equation with the viscous fluid dynamics equations and study the linear stability of the convectionless state.

 0021-9606/93/032138-06$006.00 

## II. THE FRONT PROPAGATION EQUATIONS

The fronts in the iodate–arsenous acid reaction with arsenous acid in stoichiometric excess can be described by the following reaction–diffusion equation:[7]

$$\frac{\partial c}{\partial t}=D\nabla^2 c-\alpha c(c-c_2)(c-c_3)\equiv D\nabla^2 c+f(c). \tag{1}$$

Here, $D$ is the molecular diffusivity, $c$ is the iodide concentration ($[I^-]$), $c_2$ is the initial concentration of iodate ($[IO_3^-]$), $c_3$ is the ratio of two reaction rate constants: $c_3=-k_a/k_b$ and $\alpha=k_b[H^+]^2$. The values of the reaction rate constants are given by Saul and Showalter[7] as $k_a=4.50\times10^3\ M^{-3}\ s^{-1}$ and $k_b=4.36\times10^8\ M^{-4}\ s^{-1}$. This equation is satisfied by a propagating front solution with constant speed $v_0$;

$$c(\mathbf{x},t)=c_2/(1+Be^{k(z-v_0t)}). \tag{2}$$

Here, $B$ is an arbitrary constant that specifies the position of the front. The direction of propagation is the vertical $z$ direction. The front velocity $v_0$ and the parameter $k$ are related to the chemical parameters by

$$v_0=(Dk_b/2)^{1/2}[H^+][IO_3^-]+(2D/k_b)^{1/2}k_a[H^+] \tag{3}$$

and

$$k=(k_b/2D)^{1/2}[H^+][IO_3^-]. \tag{4}$$

According to Eq. (2), the concentration of iodide is zero initially and becomes $c_2$, the initial concentration of $[IO_3^-]$, after the front passes. The density is assumed to depend linearly on the iodide concentration $c$:

$$\rho=\rho_0[1-\beta(c-c_2)]. \tag{5}$$

Here, $\rho_0$ is the density of the reacted fluid. The coefficient of linear expansion ($\beta$) is obtained from experimental measurements of the isothermal fractional density difference ($\delta$) between the unreacted and reacted fluids,[1]

$$\beta=\delta/c_2.$$

Its value is given by $\beta=1.7\times10^{-2}\ g\ cm^{-3}\ M^{-1}$. The model is made up of the reaction–diffusion equation and the fluid dynamic equations:

$$\frac{\partial \mathbf{V}}{\partial t}+(\mathbf{V}\cdot\nabla)\mathbf{V}=g\beta(c-c_2)\hat{z}-\nabla P+\nu\nabla^2\mathbf{V}, \tag{6}$$

$$\nabla\cdot\mathbf{V}=0, \tag{7}$$

and

$$\frac{\partial c}{\partial t}+\mathbf{V}\cdot\nabla c=D\nabla^2 c+f(c). \tag{8}$$

Here, $\mathbf{V}$ is the fluid velocity, $P$ is the reduced pressure and is related to the pressure by $P=p+\rho_0 gz$, $g$ the acceleration of gravity ($980\ cm\ s^{-2}$) and $\nu$ is the kinematic viscosity ($9.2\times10^{-3}\ cm^2\ s^{-1}$). The density difference is included only where it modifies the large gravity term. The convectionless state in the frame moving with the front is given by

$$\mathbf{V}^{(0)}=-v_0\hat{z},$$

$$c^{(0)}=c_2/(1+e^{kz}).$$

The origin was chosen to make $B=1$.

## III. LINEAR STABILITY ANALYSIS

We introduce small perturbations to the basic state:

$$\mathbf{V}=\mathbf{V}^{(0)}+\mathbf{V}^{(1)},$$

$$P=P^{(0)}+P^{(1)},$$

and

$$c=c^{(0)}+c^{(1)}.$$

Substituting these expressions into Eqs. (6), (7), and (8), and keeping only the terms linear in the perturbations, we obtain:

$$\frac{\partial \mathbf{V}^{(1)}}{\partial t}+(\mathbf{V}^{(0)}\cdot\nabla)\mathbf{V}^{(1)}=g\beta(c^{(1)}-c_2)\hat{z}-\nabla P^{(1)}+\nu\nabla^2\mathbf{V}^{(1)}, \tag{9}$$

$$\nabla\cdot\mathbf{V}^{(1)}=0, \tag{10}$$

and

$$\frac{\partial c^{(1)}}{\partial t}+\mathbf{V}^{(0)}\cdot\nabla c^{(1)}+\mathbf{V}^{(1)}\cdot\nabla c^{(0)}=D\nabla^2 c^{(1)}+\left.\frac{df}{dc}\right|_{c^{(0)}}c^{(1)}. \tag{11}$$

The continuity equation allows the use of a vector potential such that $\mathbf{V}^{(1)}=\nabla\times\mathbf{A}$. We are interested in the analysis of plane wave perturbations and accordingly restrict the motions to the $x$–$z$ plane. In two dimensions, we can choose the vector potential to be in only one direction $\mathbf{A}=A(x,z)\hat{y}$, where $A$ is the stream function. Taking the curl of Eq. (9) and substituting the corresponding expressions for the basic state of Eq. (11), we obtain:

$$\frac{\partial}{\partial t}[-\nabla^2 A]+v_0\frac{\partial}{\partial z}\nabla^2 A=-g\beta\frac{\partial c^{(1)}}{\partial x}-\nu\nabla^2\nabla^2 A \tag{12}$$

and

$$\frac{\partial c^{(1)}}{\partial t}=v_0\frac{\partial c^{(1)}}{\partial z}+\frac{\partial A}{\partial x}\frac{c_2 k e^{kz}}{(1+e^{kz})^2}+D\nabla^2 c^{(1)}+\left.\frac{df}{dc}\right|_{c^{(0)}}c^{(1)}. \tag{13}$$

We introduce plane wave perturbations to these equations:

$$A(\mathbf{x},t)=A(z)e^{\sigma t}\sin qx \tag{14}$$

and

$$c^{(1)}(\mathbf{x},t)=c(z)e^{\sigma t}\cos qx. \tag{15}$$

The equations now become:

$$\sigma(\nabla^2 A)=\nu\nabla^2\nabla^2 A+v_0\frac{d}{dz}\nabla^2 A-g\beta qc \tag{16}$$

and

$$\sigma c = D\nabla^2 c + v_0 \frac{dc}{dz} + qA \frac{c_2 k e^{kz}}{(q+e^{kz})^2} + \left.\frac{df}{dc}\right|_{c(0)} c. \tag{17}$$

Here, $\nabla^2 = d^2/dx^2 - q^2$. Convenient dimensionless units are defined by

$$s = \delta g/\nu D,$$

$$A = DqA',$$

$$z = z'/s^{1/3},$$

$$q = q's^{1/3},$$

$$k = k's^{1/3},$$

and

$$c = c_2 s^{1/3} c'.$$

In these units the equations are:

$$\frac{\sigma}{\nu s^{2/3}} \nabla^2 A = \nabla^2\nabla^2 A + \frac{v_0}{\nu s^{1/3}} \frac{d}{dz} \nabla^2 A - c \tag{18}$$

and

$$\frac{\sigma c}{Ds^{2/3}} = \nabla^2 c + \frac{v_0}{Ds^{1/3}} \frac{dc}{dz} + \frac{ke^{kz}}{(1+e^{kz})^2} q^2 A + \left.\frac{df}{dc}\right|_{c(0)} \frac{c}{Ds^{2/3}}, \tag{19}$$

where we have dropped the primes. This set of homogeneous equations determines an eigenvalue relation for $q$ for a given $\sigma$. These equations will be solved using a shooting method, but we shall first derive an analytical solution to compare with the numerical results.

## IV. ANALYTICAL LIMIT

In this section, we study the solution of Eqs. (18) and (19) for the case $k \to \infty$. The constant $k$ determines the thickness of the propagating front as can be seen in Eq. (2). We keep all other parameters constant including the velocity $v_0$ and the diffusivity $D$. The front velocity and the inverse thickness $k$ are related by the approximate relation $v_0 \approx kD$, obtained by neglecting the second term in Eq. (3), which proves to be very small. Consequently, in this limit, the values of $k$ and $v_0$ do not satisfy the convectionless reaction–diffusion equation [Eq. (1)] since an infinite value of $k$ would require $v_0$ to be infinite. The limit $k \to \infty$ should be considered only as an analytical solution to Eqs. (18) and (19). The result will serve as a check of the numerical method employed in the next section. The equations now have constant coefficients and the Dirac delta function replaces the derivative of the reaction term:

$$\nabla^2\nabla^2 A - (\sigma/\nu s^{2/3})\nabla^2 A - c = 0, \tag{20}$$

$$\nabla^2 c + a\frac{dc}{dz} + b_\pm c + q^2 A\delta(z) = 0. \tag{21}$$

Here,

$$a = v_0/(Ds^{1/3}) \tag{22}$$

and

$$b_\pm = \lim_{z\to\pm\infty} \frac{1}{Ds^{2/3}} \left.\frac{df}{dc}\right|_{c(0)} - \frac{\sigma}{Ds^{2/3}}. \tag{23}$$

The term containing $v_0$ in the first equation was neglected; the fact that this term is small is confirmed in the following section. The term proportional to the Dirac delta function can be replaced by a jump condition on the derivative of $c$:

$$\left.\frac{dc}{dz}\right|_{0+} - \left.\frac{dc}{dz}\right|_{0-} = -q^2 A(0). \tag{24}$$

Looking for solutions of the form $Fe^{\gamma z}$ to Eq. (21), we find:

$$\gamma_\pm = [-a \pm \sqrt{a^2 - 4(b_\pm - q^2)}]/2. \tag{25}$$

The jump condition given in Eq. (24) and the requirement that the solution vanish for $z \to \pm\infty$ gives

$$c = \begin{cases} Fe^{\gamma_- z}, & \text{if } z > 0, \\ Fe^{\gamma_+ z}, & \text{if } z \leqslant 0, \end{cases} \tag{26}$$

where

$$F = \frac{2q^2 A(0)}{\sqrt{a^2 - 4(b_+ - q^2)} + \sqrt{a^2 - 4(b_- - q^2)}}. \tag{27}$$

We are now left with a single linear homogeneous equation for $A$:

$$\nabla^2\nabla^2 A - (\sigma/\nu s^{2/3})\nabla^2 A + Fe^{\gamma_\pm z} = 0 \tag{28}$$

with the corresponding value of $\gamma$. Without loss of generality we can require that $A(0) = 1$ and write a general solution as a sum of a particular solution plus two linearly independent solutions to the homogeneous equation. This leads to the general form for $A$:

$$A = \begin{cases} f_1 e^{q_1 z} + f_2 e^{q_2 z} + g_+ e^{\gamma_+ z}, & \text{if } z \leqslant 0, \\ f_3 e^{-q_1 z} + f_4 e^{-q_2 z} + g_- e^{\gamma_- z}, & \text{if } z > 0. \end{cases} \tag{29}$$

The coefficients $g_\pm$ are given by

$$g_\pm = F/(\gamma_\pm^4 - 2q^2\gamma_\pm + q^4). \tag{30}$$

The values of the constants $f_i$ are obtained by requiring the solution to be continuous up to the third derivative and to satisfy the value of $A(0)$ chosen. This is equivalent to requiring a vanishing determinant of the matrix:

$$\begin{pmatrix} 1 & 1 & -1 & -1 & -g_+ + g_- \\ q_1 & q_2 & q_1 & q_2 & -g_+\gamma_+ + g_-\gamma_- \\ q_1^2 & q_2^2 & -q_1^2 & -q_2^2 & -g_+\gamma_+^2 + g_-\gamma_-^2 \\ q_1^3 & q_2^3 & -q_1^3 & -q_2^3 & -g_+\gamma_+^3 + g_-\gamma_-^3 \\ 1 & 1 & 0 & 0 & 1 - g_+ \end{pmatrix}.$$

This determinant gives an analytical equation for the unknown eigenvalue $q$ that can be solved using standard numerical techniques. The results are evaluated numerically for the mixture used in the experiments of McManus *et al.* The composition of this mixture is: $[IO_3^-] = 5\times10^{-3}$ M, $[H_3\,AsO_3] = 29.8\times10^{-3}$ M, $[H^+] = 10\times10^{-3}$ M. The molecular diffusivity is $D = 2.0\times10^{-5}$ cm$^2$ s$^{-1}$. In Fig. 1, we show the dependence of the growth rate $\sigma$ on the wave number of the perturbation $q$ in dimensional units. The unit conversion is obtained by multiplying the wave number $q$ in our units by $s^{1/3}$. The growth rate $\sigma$ is already in

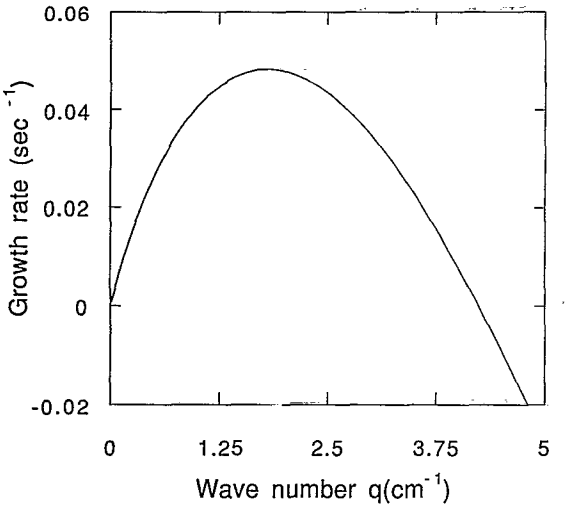


FIG. 1. The variation of the growth rate $\sigma$ with the wave number perturbation $q$. This relation follows from the thin front approximation of Sec. IV. The critical value of the wave number for marginal stability ($\sigma=0$) is $q_c=4.244\ \mathrm{cm}^{-1}$.

$s^{-1}$. The growth rate is positive for small wave numbers implying instability with respect to large wavelength perturbations. There is a critical wave number $q_c$ at which the growth rate is equal to zero and for values $q>q_c$ it is negative. Although the qualitative features of the $\sigma$–$q$ relation are the same as the one obtained previously with the eikonal relation,[3] the quantitative features are different. For example, the critical wave number in the $k\to\infty$ theory is equal to $q_c=4.244\ \mathrm{cm}^{-1}$ whereas using the eikonal relation gives $q_c=48.74\ \mathrm{cm}^{-1}$. These results show that the $k\to\infty$ limit is essentially different from the eikonal approximation. The reason is that the $k\to\infty$ limit assumes that other quantities, such as the front velocity, remain constant instead of varying with $k$, and therefore is not a realistic thin front approximation.

## V. THE FRONT OF FINITE THICKNESS

Here we find the eigenvalue $q$ of Eqs. (18) and (19) using a shooting method[12] for finite $k$. This method is commonly used to obtain the eigenvalues for ordinary differential equations (ODE's) involving two-point boundary value problems. The method consists of starting the numerical solution at one boundary point with the initial conditions prescribed by the problem plus some additional trial conditions. The boundary values at the second point are obtained by changing the trial conditions at the first point and choosing the correct eigenvalue. In our case, Eqs. (18) and (19) can be transformed into a system of six first-order ODE's of the form:

$$\frac{d}{dz}\Psi=M\Psi, \tag{31}$$

where

$$\Psi=\begin{pmatrix}\Psi_1\\ \Psi_2\\ \Psi_3\\ \Psi_4\\ \Psi_5\\ \Psi_6\end{pmatrix}=\begin{pmatrix}A\\ dA/dz\\ c\\ d^2A/dz^2\\ d^3A/dz^3\\ dc/dz\end{pmatrix} \tag{32}$$

and $M$ is a $6\times6$ matrix with the corresponding functions of $z$ as entries. The boundary conditions require that $c$, $A$, and $dA/dz$ vanish as $z\to\pm\infty$. In the algorithm the limits are replaced by taking the boundaries as two points $z=\pm z_m$ with large absolute values. At each of the boundaries we have three free parameters to choose: $d^2A/dz^2$, $d^3A/dz^3$, and $dc/dz$. We have a total of six free parameters to start shooting toward $z=0$, three at each boundary. We have to pick the free parameters and the eigenvalue $q$ to match the solutions at $z=0$. This procedure is simplified by using the fact that the system of ODE's is linear. Any solution that satisfies the boundary conditions at a given point is a linear combination of the solutions obtained with the initial conditions:

$$\begin{pmatrix}\Psi_4\\ \Psi_5\\ \Psi_6\end{pmatrix}=\begin{pmatrix}1\\0\\0\end{pmatrix},\quad \begin{pmatrix}0\\1\\0\end{pmatrix}\quad\text{and}\quad\begin{pmatrix}0\\0\\1\end{pmatrix}, \tag{33}$$

where these functions are evaluated at the boundaries. We label each solution as $\Psi_i^{\pm}(z)$ for $i=1,2,3$; the superscript $+$ $(-)$ corresponds to the solution that started at $+z_m$ $(-z_m)$. Accordingly, any function that satisfies the boundary conditions at $+z_m$ is a linear combination of the functions $\Psi_i^+$. This linear combination is matched with the linear combination that started from $-z_m$. This leads to

$$x_1\Psi_1^+(0)+x_2\Psi_2^+(0)+x_3\Psi_3^+(0)$$
$$=y_1\Psi_1^-(0)+y_2\Psi_2^-(0)+y_3\Psi_3^-(0), \tag{34}$$

which is a homogeneous system of six equations in the variables $x_i$ and $y_i$. The eigenvalue $q$ is obtained by requiring that the determinant of this system vanish.

## VI. RESULTS

This method was applied first to large values of $k$. The implicit Euler method was chosen to shoot from the boundaries $\pm z_m$ to avoid numerical instabilities. For large values of $k$, the coefficients resemble Dirac-delta functions. They are highly peaked at $z=0$ and are negligible elsewhere, requiring the use of a very fine partition around this point. It was convenient to introduce additional intermediate points, $z=\epsilon$ and $z=-\epsilon$ with matching conditions similar to the ones described on the previous section. A very fine partition was introduced in the interval $[-\epsilon,+\epsilon]$ with the typical value of $\epsilon$ being $50/k$. For very large $k$ [$k=1.3\times10^6$ compared to the value of $k=2.133$ obtained from the experimental conditions[1] and Eq. (4) expressed in dimensionless units], the dependence of the growth rate $\sigma$ on the wave number $q$ agrees with the analytical results up to three significant figures. The resulting trace for $\sigma-q$ in Fig. 1 is indistinguishable from the analytical results for $k\to\infty$. The analytical value of $q_c$ is $4.244\ \mathrm{cm}^{-1}$ while the

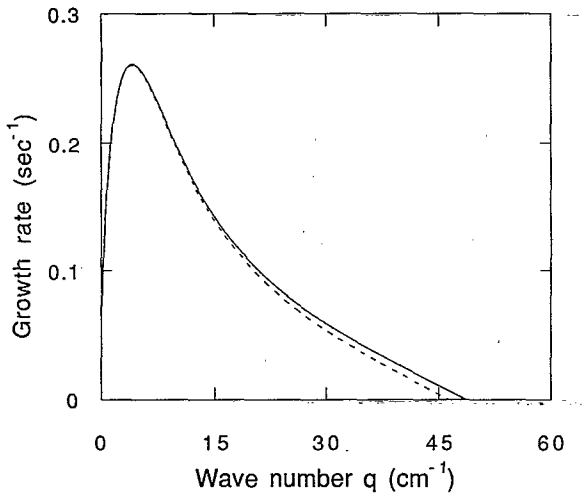


FIG. 2. The variation of the growth rate $\sigma$ with the perturbation wave number $q$. The solid trace corresponds to the eikonal approximation for the front propagation. The broken trace corresponds to the one variable reaction–diffusion equation. The composition of the mixture is: $[IO_3^-]=5\times10^{-3}$ M, $[H_3\,AsO_3]=29.8\times10^{-3}$ M, $[H^+]=10\times10^{-3}$ M. The molecular diffusivity is $2.0\times10^{-5}$ cm$^2$ s$^{-1}$.

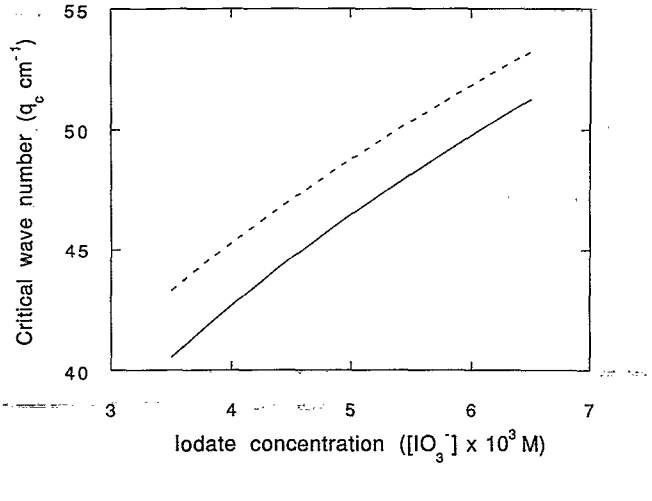


FIG. 3. The critical wave number $q_c$ as a function of the iodate concentration. The solid trace is the result obtained with the reaction–diffusion equation. The broken trace indicates the result obtained with the eikonal relation.

value obtained with the shooting method is 4.240 cm$^{-1}$. This result confirms the accuracy of the shooting method. In the treatment for $k\rightarrow\infty$, we neglected the term proportional to $v_0$ in Eq. (18). If the term is kept the answer for $q_c$ would be 4.236 cm$^{-1}$, very close to the analytical value where the term was neglected. The same small error is introduced in the calculation of the $\sigma$ vs $q$ plot.

The shooting method applied to fronts of finite thickness leads to results that are close to the results of the eikonal approximation. In Fig. 2, we compare the results of the shooting method with the ones obtained with the eikonal approximation. The chemical composition chosen corresponds to the McManus experiments[1] as was previously described. The agreement is good overall, and is best near $q=0$. This is likely due to a decrease in the curvature of the perturbation as the wavelength is increased, indicating that the eikonal relation is a better approximation for smaller curvatures. The critical wave number $q_c=48.74$ cm$^{-1}$ obtained using the eikonal relation is in good agreement with $q_c=46.39$ cm$^{-1}$ from the reaction–diffusion equation. The speed of the front obtained from the reaction–diffusion equation ($v_0=3.31\times10^{-3}$ cm s$^{-1}$) is slightly higher than the experimental convectionless front ($v_0=2.95\times10^{-3}$ cm s$^{-1}$). Modifying the parameter $k_b$ to fit the experimental speed ($k_b=3.45\times10^8$ M$^{-4}$ s$^{-1}$) results in a value of $q_c=46.01$ cm$^{-1}$ for the critical wave number. Since this modification changed the results by only a small fraction, we will continue our analysis with the rate constants provided by Saul *et al.*

The reaction–diffusion equation allows us to investigate the onset of convection in different chemical mixtures. In Fig. 3 we plot the critical wave number $q_c$ as a function of the concentration of iodate ($[IO_3^-]$) and compare it with the results obtained with the eikonal relation. The range where the chemical concentration is varied ($3.5$–$6.0\times10^{-3}$ M) is a reasonable extension of the range explored in petri dish experiments ($4.2$–$5.0\times10^{-3}$ M). The change in $q_c$ observed from the eikonal relation is due to the change in the fractional density difference between the reacted and unreacted fluids. It is assumed that the fractional density difference is proportional to the iodate concentration. This assumption is justified from the fact that in reactions with an excess of arsenous acid almost all iodate is transformed into iodide as the front passes. In contrast to the eikonal relation, the reaction–diffusion equation not only accounts for the change in density but also for the change in speed and thickness of the chemical wave. The dependence of $q_c$ obtained from the reaction–diffusion equation is almost identical to the one obtained from the eikonal relation with the exception of a shift between the curves. We attribute this result to the important role played by the density difference on the hydrodynamic instability of the front. For both cases the critical wave number increases as the iodate concentration increases, corresponding to an increase in the fractional density difference. The increase in the critical wave number implies that smaller wavelengths can trigger the instability, thus making the front more unstable. These results indicate that the greater the density difference, the more unstable the convectionless front becomes. In Fig. 4 we calculate $q_c$ as a function of the hydrogen ion concentration ($[H^+]$). In this case there is no change in the density difference between the unreacted and reacted fluids since we keep the iodate concentration constant. The only other factors involved in the variation of $q_c$ are the speed and the thickness of the front. An increase in the concentration of the hydrogen ion corresponds to an increase in the critical wave number (more unstable). The increase in hydrogen makes the front thinner, so the thinner the front the more unstable it becomes. The eikonal relation provides only a very weak dependence of $q_c$ on the speed of the front and none as a function of the front thickness. Consequently the eikonal relation gives $q_c$ independent of $[H^+]$.

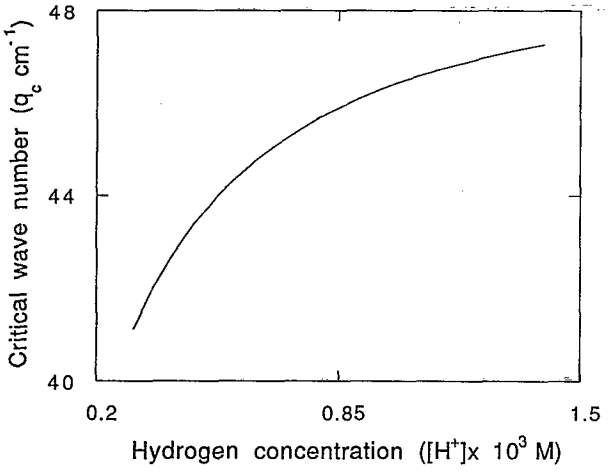


FIG. 4. The critical wave number $q_c$ as a function of the hydrogen ion concnetration ([$H^+$]).

Hence, the inclusion of the reaction–diffusion equation in the theory yields an observable variation of $q_c$ with [$H^+$], not obtainable with the eikonal approximation.

## VII. CONCLUSIONS

The linear stability analysis of chemical waves in the iodate–arsenous reaction shows instability for perturbations whose wavelengths are greater than a critical wavelength ($\lambda_c=2\pi/q_c$) as the waves propagate upward. This critical wavelength depends not only on the density difference between reacted and unreacted fluids but also on the thickness and speed of the chemical front. For the iodate–arsenous reaction with excess of arsenous acid, the wavelength $\lambda_c$ is well approximated by replacing the reaction–diffusion mechanism by the eikonal relation.

Experiments in the iodate–arsenous system show no convection in cylinders of diameter less than 0.94 mm. An estimate for the critical diameter for onset of convection based on the present results should lie between half the critical wavelength and the critical wavelength: [0.68,1.36] mm. A detailed calculation of the critical diameter should include the boundary conditions at the walls and the correct treatment of the cylindrical geometry. A previous theoretical work[13] based on the eikonal relation indicates a transition to nonaxisymmetric convection for a critical diameter of 1.14 mm. The agreement between the eikonal relation and the reaction–diffusion theory reaffirms this result.

The present work shows that the instability may be driven by changing the chemical composition of the mixture instead of using cylinders of different diameter. This may facilitate future comparisons between theory and experiment. The numerical method described may be extended to study the hydrodynamic stability of other propagating fronts, such as the ones in the iron–nitric acid system or the Belousov–Zhabotinskii reaction.

## ACKNOWLEDGMENTS

Discussions with Kenneth Showalter, John Ringland, and Jie Huang are gratefully acknowedged. This work is supported in part by the National Science Foundation Grant No. RII-8922106 and the National Research Center for Coal and Energy.

[1] T. McManus, Ph.D. thesis, West Virginia University, Chap. 3, 1989.
[2] J. A. Pojman, I. R. Epstein, T. J. McManus, and K. Showalter, J. Phys. Chem. **95**, 1299 (1991).
[3] B. F. Edwards, J. W. Wilder, and K. Showalter, Phys. Rev. A **43**, 749 (1991).
[4] D. A. Vasquez, B. F. Edwards, and J. W. Wilder, Phys. Rev. A **43**, 6694 (1991).
[5] J. P. Keener, SIAM J. Appl. Math. **46**, 1039 (1986).
[6] J. W. Wilder, D. A. Vasquez, and B. F. Edwards (to be published).
[7] A. Saul and K. Showalter, in *Oscillations and Traveling Waves in Chemical Systems,* edited by R. J. Field and M. Burger (Wiley, New York, 1985), p. 419.
[8] J. P. Keener and J. J. Tyson, Physica D **32**, 307 (1988).
[9] A. Hanna, A. Saul, and K. Showalter, J. Am. Chem. Soc. **104**, 3838 (1982).
[10] J. W. Wilder, B. F. Edwards, and D. A. Vasquez, Phys. Rev. A **45**, 2320 (1992).
[11] B. F. Edwards, D. A. Vasquez, and J. W. Wilder (to be published).
[12] W. Press, B. Flannery, S. Teukolsky, and W. Vetterling, *Numerical Recipes* (Cambridge U.P., Cambridge, 1986).
[13] D. A. Vasquez, B. F. Edwards, and J. W. Wilder, Phys. Fluids A **4**, 2410 (1992).